eurofins | EAG Laboratories

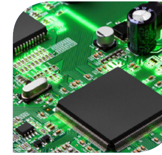
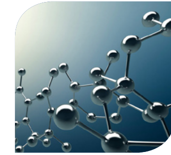

Applications of 4D-STEM in Materials Characterization

Measuring nanoscale structural and electrostatic properties of materials using 4D-STEM.

Introduction

Scanning transmission electron microscopy (STEM) is an essential tool in materials characterization providing both high resolution imaging and spectroscopy when coupled with energy-dispersive x-ray and electron energy loss detectors. During regular STEM imaging, a diffraction pattern from the converged probe is projected onto detectors below the sample and images are constructed by integrating large portions of the diffraction pattern to generate one intensity value per probe position; the image is constructed one pixel at a time by raster scanning the probe across the sample. This integration process discards vast amounts of information contained in the diffraction pattern about the sample's structural and electrostatic properties. However, the development of fast cameras synchronized with the scanning probe has led to the wide adoption of four-dimensional STEM (4D-STEM), where a diffraction pattern is captured for every probe position in the raster scan. This allows us to capture all the information available from the probe's interaction with the sample and then use computational analysis to measure the sample's properties. This process is illustrated schematically in Figure 1.

In this application note, we will focus on three applications of 4D-STEM: orientation mapping, strain analysis, and electric field imaging. However, 4D-STEM is an exceptionally flexible technique; different electron probe conditions and data analysis methods enable a wide variety of measurements of other properties, including polarization, charge density, structural/chemical ordering, and local symmetry, among others. For full reviews of 4D-STEM methods and possible applications, please refer to the following articles [1-4].

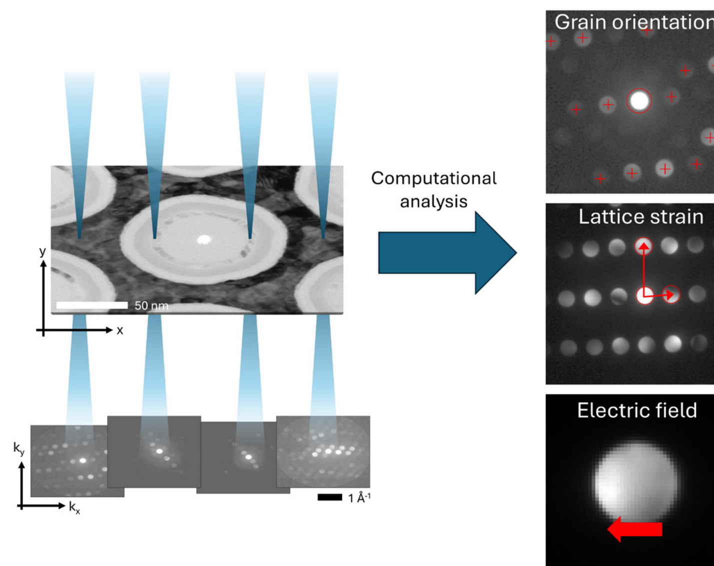

Figure 1: An overview of three 4D-STEM techniques available at EAG.

Orientation Mapping

The orientation and size of grains in a polycrystalline material can have a significant impact on its properties and performance. The orientation of an individual grain is reflected in an electron diffraction pattern through the position and relative intensity of the diffracted disks. While conventional TEM techniques such as selected area electron diffraction and dark field TEM imaging can precisely identify grain orientation or highlight individual grains in imaging, respectively, neither of these techniques does both at the same time. 4D-STEM is capable of both identifying orientation and constructing a grain map simultaneously with automated orientation mapping. When a 4D STEM dataset is collected from a polycrystalline material, the diffraction pattern for each probe position will reflect the local crystal orientation that the probe passed through. By matching the positions of the diffracted disks to a database of simulated diffraction patterns generated from a wide range of crystal orientations, we can identify the orientation of each pixel.

To demonstrate this process, we collected a 4D-STEM dataset from a 3D NAND device and mapped the orientation within the metallic W gate layer. A virtual BF-STEM image generated by integrating the center disk in the 4D data is shown in Figure 2a; the colored dots indicate the positions where the diffraction patterns in Figure 2b were extracted. The variations of these patterns clearly show the polycrystalline nature of the gate. The positions of the center disk and all diffraction disks in Figure 2b are located by cross correlation and highlighted in the respective colors. Matching the disk positions with the database generated from the W crystal structure (cubic, $Im\bar{3}m$ space group) allows us to construct the orientation maps shown in Figures 2c and 2d. Figure 2c shows the grain orientation along the x-direction (in-plane) and Figure 2d shows the grain orientation along the z-direction (out-of-plane), as indicated by the axes on Figure 2a. Having both the x and z orientation uniquely defines the orientation of the pixel. In the orientation maps, the colors correspond to the inverse pole figure shown on the far right which maps each color to a specific Miller index for the W crystal structure. For example, a red colored pixel in Figure 2c in the map indicates that the [001] axis of W is aligned close to the x-direction in that region. Black pixels indicate that there was no strong correlation between the diffraction pattern and the database, indicating that the pixel is either amorphous, as is the case for the SiO_2 and SiN layers of the device, or has a different crystal structure not in the database, as is the case for the poly-Si layer. The correlation strength can be used to assess the degree of crystalline ordering of the material.

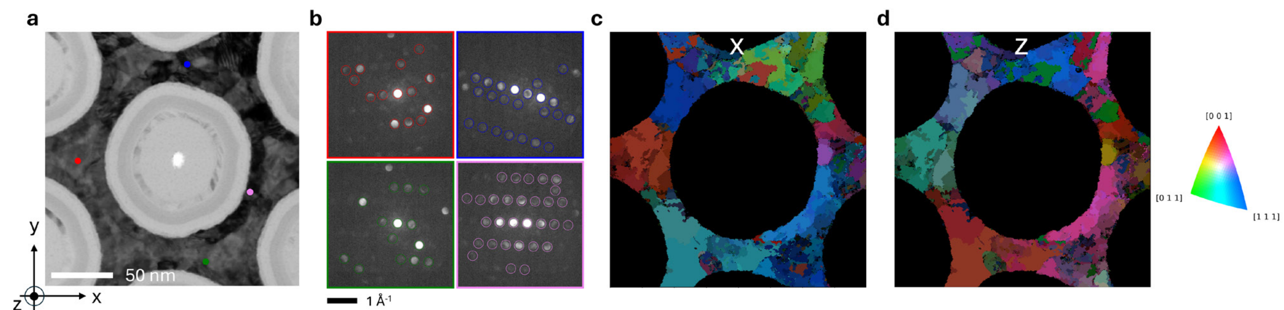

Figure 2: ***a*** *A virtual BF image of a 3D NAND device.* ***b*** *Diffraction patterns extracted from a at the positions marked.* ***c***, ***d*** *In-plane (**c**) and out-of-plane (**d**) orientation maps of the W layer.*

In 4D STEM, grain orientation is generally a continuous measurement, so the orientation assigned to a pixel can be any value between the directions indicated in the inverse pole figure. However, in Figures 2c and 2d, we have clustered together pixels where the orientation differs by less than 5 degrees and assigned them to a single average orientation of the region; this is how we identify discrete crystalline grains from the continuous orientation map. Using the clustered grains, we can calculate the grain size as the equivalent diameter of each cluster. The grain size

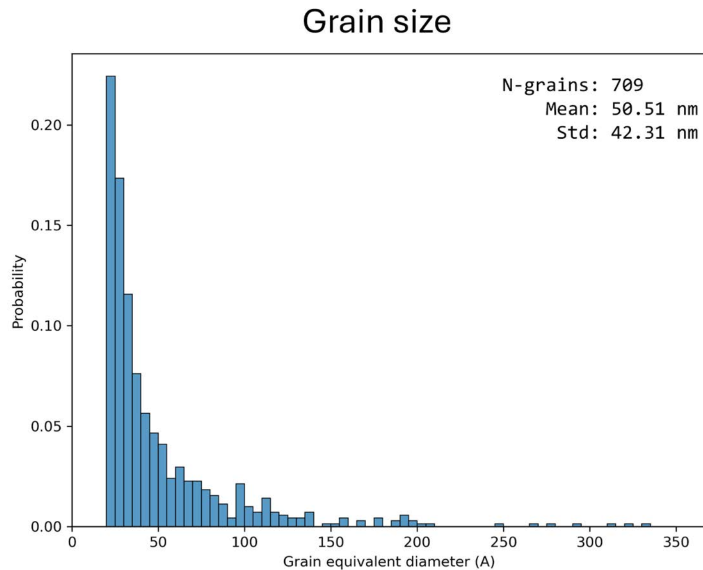

Figure 3: Grain size analysis based on orientation mapping in figures 2c and 2d.

histogram and statistics of the grain size distribution are shown in Figure 3. Here, we've used a minimum grain size of 20 Å, equivalent to 4 pixels, to avoid very small grains which are more likely affected by noise.

Strain Analysis

Strain engineering in epitaxial thin films is an important tool for scientists and engineers to elicit the desired behavior from their film. The interplay of strain and composition at epitaxial interfaces directly leads to the mechanical and electrical properties that determine overall performance. The strain in the atomic structure of a material is reflected in the diffraction pattern as slight displacement of the diffraction disk position compared to the unstrained structure. Therefore, we can use 4D-STEM to construct a strain map of a sample by precisely measuring the position of all diffraction disks in each diffraction pattern and comparing them to reference values.

We have collected 4D STEM data from a III-V heterostructure extracted from a commercial LED sample. The device consists of alloyed (In/Al)GaN layers epitaxially grown on top of GaN, as shown in the HAADF image in Figure 4. In Figure 4, the bottom of the device is on the left and the top is on the right. The InGaN layers are grouped into superlattice (SL) and multiple quantum well (MQW) structures and the barrier AlGaN layers appear near the top of the stack. Although the alloying of In/Al with Ga in these devices is the primary mechanism for modifying the local band gap, strain in the lattice can also have an effect on the band gap via the piezoelectric effect. Therefore, fine tuning both the strain and composition of the heterostructure is important in ensuring the performance of the device. The four components of the strain tensor, ε_{xx} (growth direction), ε_{yy} (in-plane), ε_{xy} (shear), and θ (rotation) are also shown in Figure 4. As expected for these types of devices, most of the strain appears along the growth direction in the absence of any defects. Pure InN has a higher lattice constant than GaN, so InGaN quantum wells exhibit tensile strain. Pure AlN has a smaller lattice constant than GaN, so AlN layers exhibit compressive strain. Maps of the other components exhibit very low contrast because there is little lattice distortion in the other dimensions.

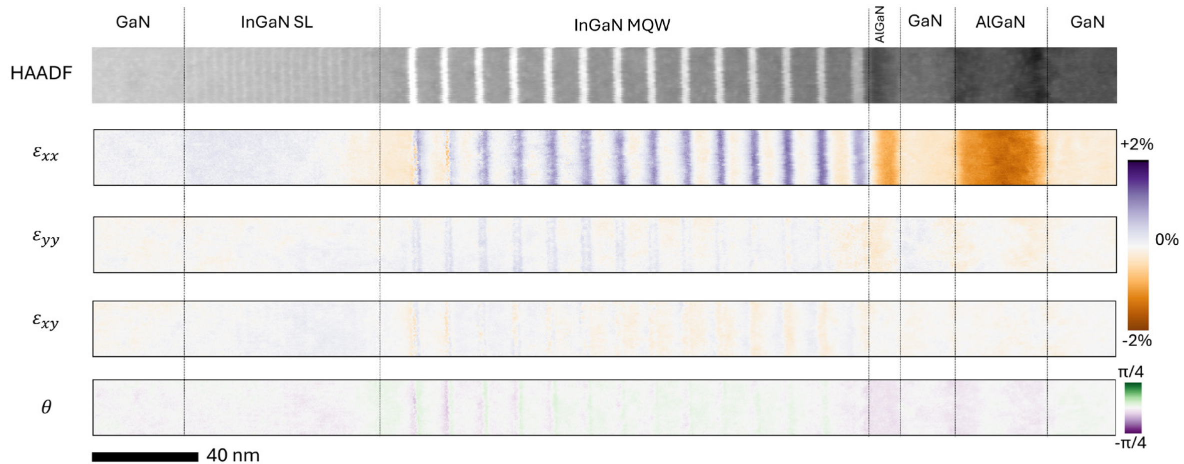

Figure 4: Strain analysis of a III-V LED device. The field of view covers InGaN SL/MQW regions and alternating GaN and AlGaN layers. The bottom of the device is on the left and the top is on the right.

Electric Field Imaging

In addition to the structural information that can be derived from the diffracted disks, the center disk of the diffraction pattern also carries information about the electrostatic properties of the material. As the electron beam passes through the sample, it interacts with the local electric field via the Lorentz force; this is reflected in the diffraction pattern as a shift in the intensity distribution of the center disk. Figure 5a illustrates an example of this process; here, the electric field in the sample points to the right, so as the electron beam passes through, it is shifted to the left and the center disk appears brighter on the left side. This shift in the intensity distribution is measured by calculating the intensity-weighted average position of the center disk, also referred to as the center of mass (**COM**). The **COM** vector can be calibrated to reveal the electric field in the sample based on the beam condition. Calculating the **COM** for every diffraction pattern in a 4D STEM data set allows us to calculate the electric field vector for every pixel. The electric field measured with this method reveals only the two-dimensional (x/y) electric field vector projected along the depth of the sample. The full electric field, including out-of-plane (z) components, can be constructed by preparing multiple samples with known orientation relationships.

The same LED device is also a good sample to demonstrate electric field imaging. For this case, we will focus just on the SL and MQW regions shown in Figure 5b. The epitaxial layers in the LED exhibit a strain induced piezoelectric polarization caused by the lattice mismatch between layers. This generates a piezoelectric field at the InGaN-GaN interfaces which can change the local band gap and adversely affect the performance of the device. Directly imaging the piezoelectric field with 4D-STEM can aid in the development of growth techniques that work to mitigate this effect. An image of the x-component of the electric field (Ex) is shown in Figure 5c and the associated line profile is shown in Figure 5d. The red color in Figure 5c indicates regions where Ex points left, and the blue color indicates regions where Ex points right. The strong alternating E-fields correspond with the edges of the InGaN quantum wells.

It is also interesting to note that the InGaN layers in the SL region are visible in the E-field image in Figures 5c and 5d whereas they are not visible as distinct features in strain map in Figure 4. The difference indicates that these quantum wells generate very little lattice distortion but still generate an electrostatic field like the thicker quantum wells in the MQW region. This highlights the importance of examining both structural and electrostatic properties of the sample.

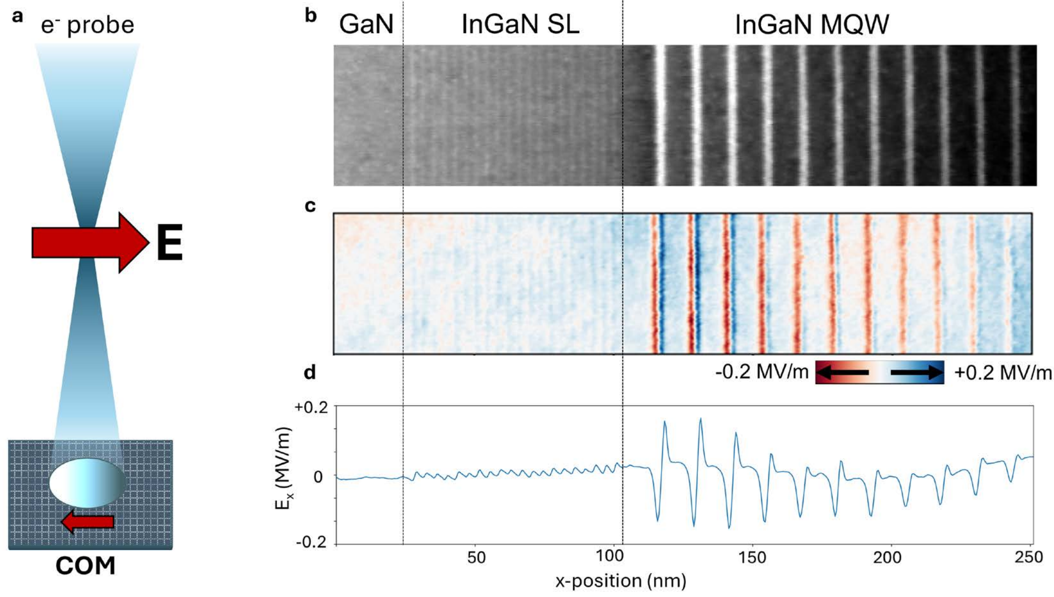

Figure 5: ***a*** *A schematic illustrating the electric field imaging process.* ***b*** *A HAADF image from an LED device covering the SL and MQW regions.* ***c, d*** *The x-component of the electric field (****c****) and the line profile averaged along the vertical direction (****d****).*

Comparison with Precession Electron Diffraction (PED)

The 4D-STEM applications discussed here overlap Precession electron diffraction (PED), another STEM technique which is also available at Eurofins EAG [5]. Although PED was offered commercially several years before 4D-STEM was widely adopted, PED can be classified as a specialized 4D-STEM experiment. In PED, diffraction patterns are collected as the beam scans, just as in 4D-STEM, however the electron beam is also simultaneously precessed (rotated) around the optical axis during the scan. Precessing the beam allows for a range of diffraction conditions to be captured in the final diffraction pattern at each probe position, whereas only one diffraction condition is captured in regular 4D-STEM. This generates a diffraction pattern with less dynamical artifacts and a larger number of disks, enabling more precise determination of orientation and strain. However, this comes at the cost of spatial resolution and scanning speed. While 4D-STEM strain/orientation mapping can resolve features down to ~2 nm depending on the sample structure and probe conditions, PED spatial resolution is limited to 5-10 nm. The increased scanning speed available in a regular 4D-STEM experiment also means that there is more flexibility to cover larger fields of view or to scan with a smaller step size. In addition, our 4D-STEM analysis is implemented with custom software which means we have the flexibility to combine a variety of measurements and adapt to a wider variety range of samples and beam conditions that may not be feasible for commercial PED software. For example, strain mapping and E-field measurements can be generated from the same 4D-STEM dataset, which is not possible in PED.

Conclusion

4D-STEM is a powerful tool for materials characterization that can be used to measure a broad range of material properties. In this application note, we have covered three applications of 4D-STEM for measuring structural and electrostatic properties in semiconductor materials. Eurofins EAG provides our customers with access to state-of-the-art electron microscopy facilities and expertise to deliver the highest quality imaging data. As demonstrated here, we also offer advanced microscopy techniques and software tools to perform complex measurements that require cutting-edge data acquisition and analysis methods. As the field of microscopy and its applications are continually expanding, we also offer technical development services to help our customers solve their most challenging materials science problems that may not have an off-the-shelf solution. Contact us today to learn how we can help with your next project.

References

[1] C. Ophus, “Four-Dimensional Scanning Transmission Electron Microscopy (4D-STEM): From Scanning Nanodiffraction to Ptychography and Beyond”. Microscopy and Microanalysis 25, 563-582 (2019).

[2] C. Addiego, W. Gao, H. Huyan, X.Q. Pan, “Probing charge density in materials with atomic resolution in real space”. Nature Reviews Physics 5, 117-132 (2023).

[3] K.C. Bustillo, S.E. Zeltman, M. Chen, J. Donohue, J. Ciston, C. Ophus, A.M. Minor, “4D-STEM of Beam-Sensitive Materials”, Accounts of Chemical Research 54, 2543-2551 (2021).

[4] B. H. Savitzky et al, “py4DSTEM: A Software Package for Four-Dimensional Scanning Transmission Electron Microscopy Data Analysis”, Microscopy and Microanalysis 27, 712-743 (2021).

[5] https://www.eag.com/app-note/material-structural-analysis-power-of-ped-at-nanometer-scale/

Copyright © 2025 Eurofins Scientific | Rev. 03.18.25 | M-084225